About the relevance of roughness parameters used for characterizing worn femoral heads

D. Najjar[a,*], M. Bigerelle[a,b], H. Migaud[c], A. Iost[a]

[a]*Laboratoire de Métallurgie Physique et Génie des Matériaux, UMR CNRS 8517, ENSAM, Equipe Surfaces et Interfaces, 8 Boulevard Louis XIV, 59046 Lille, Cedex, France*
[b]*Laboratoire Roberval, FRE 2833, UTC/CNRS, Centre de Recherches de Royallieu, BP20529-60205 Compiègne, France*
[c]*CHRU Lille, Service d'Orthopédie C, Hôpital Roger Salengro, 59037 Lille, Cedex, France*

Abstract

This study aims to contribute to the definition of a methodology, which can help to select a relevant roughness parameter with a view to describing the topography of orthopaedic bearing surfaces. In this investigation, the surface topography of a retrieved titanium alloy (TA6V) femoral head was characterized using visual inspection, optical microscopy and three-dimensional contacting profilometry. A numerical analysis of roughness measurements was then undertaken to assess in a first step the values of different roughness parameters of interest found in papers dealing with the topography of orthopaedic bearing surfaces. In a second step, the Analysis of Variance (ANOVA) and the Computer-Based Bootstrap Method were combined to determine statistically, and without preconceived opinion, which of those parameters is the most relevant to describe the different investigated worn regions of the studied femoral head.

1. Introduction

For the last 30 years, the most implanted prostheses consist of a hard metallic or ceramic femoral head articulating against an ultra-high molecular weight polyethylene (UHMWPE) acetabular cup. Despite the growing success of this type of surgery, limiting the wear of UHMWPE components remains a key issue to improve the long-term performance of these Charnley type prostheses. While the influence of variations in component design, in surgical technique and/or in patient activity level cannot be ignored, the scratching of the metallic femoral head is currently thought to be a major factor affecting the wear rate of the UHMWPE counterface [1–10]. This scratching phenomenon is increasingly suspected to be caused by hard third bodies such as particles of bone, cement and/or metal, which have often been found embedded in acetabular cups and in the peri-prosthetic tissues [1–5,11,12]. This concern has to be especially taken into consideration when using contemporary constructs with modular interfaces and/or porous metal coatings that are likely to liberate hard metal debris.

As far as the correlation between scratching of femoral heads and the wear of UHMWPE components is concerned, discrepancies have been observed between the quantitative results of different laboratory wear tests and clinical observations [2,3,6–9]. These discrepancies have mainly been attributed to the fact that, in clinical situations, localized head scratching may occur and generate damaged regions whose sites, size and severity magnitude are seemingly randomly distributed [2,3,7,10]. These discrepancies are all the more difficult to interpret that, as claimed by Hall et al. [2], considerable work still needs to be undertaken in terms of specifying which relevant roughness parameter should be used in assessing surface texture of femoral heads in relation to the wear of UHMWPE components.

Among the various studies carried out on biomaterials for the last 20 years, any roughness parameter has

---
*Corresponding author. Tel.: +33 320 622 765; fax: +33 320 622 957.
E-mail address: denis.najjar@lille.ensam.fr (D. Najjar).

universally been admitted for describing the topography of orthopaedic bearing surfaces. Even if the arithmetic roughness parameter R_a is the one parameter which has systematically been used in these studies, the root mean square roughness R_q, the total amplitude R_t, the peak height R_p, the mean peak height R_{pm} and the skewness S_k of the amplitude distribution function (ADF) have been also considered but in a lesser extent [1,2,5,10]. Consequently to an analysis of the limits of the aforementioned roughness parameters, Hall et al. have proposed in 1997 that further investigation of the parameters derived from the bearing area curve (BAC) is urgently required [2]. Unfortunately, up to now, no results related to this interesting idea have been found in the literature by the authors.

This study aims to present a generic methodology that can help to determine quantitatively, and without any preconceived opinion, which relevant roughness parameter(s) among the aforementioned ones should be used in assessing the surface topography of femoral heads in relation to the wear of UHMWPE components. Illustrated in the case of a retrieved titanium alloy femoral head showing distinct worn regions visible at naked-eye after revision surgery, this generic methodology makes the most of the power of modern computers combining the conventional Analysis of Variance (ANOVA) and the recent and powerful statistical Computer-Based Bootstrap Method (CBBM).

2. Experimental methods

2.1. Clinical information and visual inspection results after surgery

The articulating components under investigation were retrieved after 4 years and 5 months because of the detection of an osteolysis phenomenon (without loosening) on the survey radiographs of the patient. During the period of implantation, the UHMWPE acetabular liner was inserted in a Harris–Galante Mark I metallic shell and the 28 mm diameter metallic femoral head was mounted on a cemented femoral stem.

Since the foreign third bodies are increasingly suspected of being the dominant cause of the scratch generation, this titanium alloy (TA6V) femoral head (Fig. 1a) was especially selected because an embedded metallic fiber was detected in the UHMWPE counterface after revision surgery (Fig. 1b). This centimeter-length foreign body came from the titanium fibermesh, which was deposited on the Harris–Galante metallic cup during the fabrication process. It must be pointed out that polyethylene and metallic debris were detected by histological analyses on the peri-prosthetic tissues.

The influence of this foreign body on the degradation mechanisms of both the retrieved UHMWPE acetabular liner and titanium alloy femoral head have already been studied in previous papers [12,13]. As far as the degradation of the titanium alloy femoral head is concerned, three kinds of regions were distinguished by visual inspection at its surface (Fig. 1c):

- Regions covering about 30% of the entire surface and visually having a bright finish. These regions noted LS (for lightly scratched) are white-colored in Fig. 1c.
- Regions covering between 10% and 20% of the entire surface and visually having a low brightness level. Two regions of this type were detected along a meridian; a region located near the polar region and another one located near the equatorial region. These regions respectively noted severely scratched polar region (SSPR) and severely scratched equatorial region (SSER) are dark gray-colored in Fig. 1c.
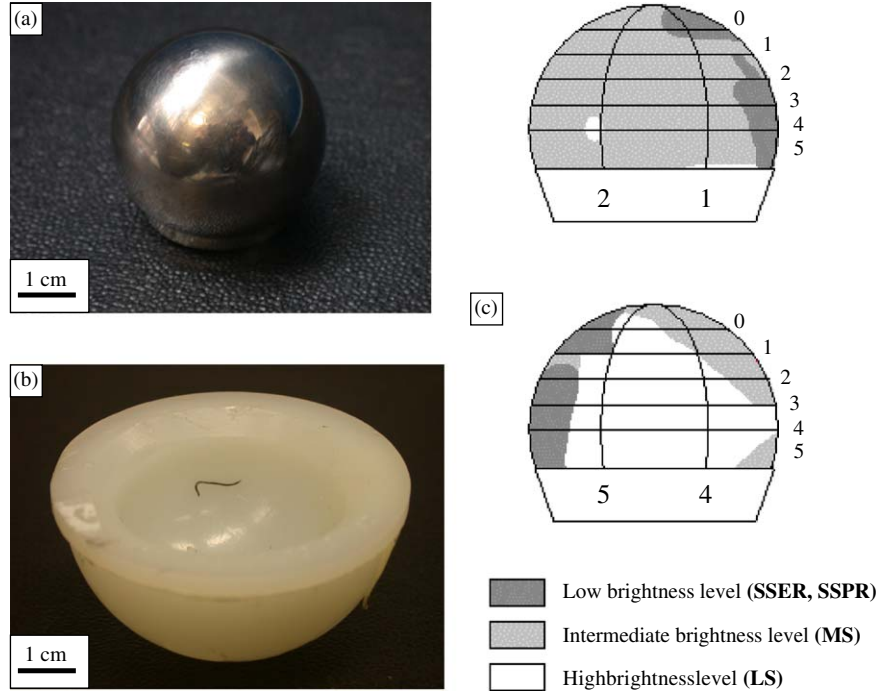
Fig. 1. (a) Retrieved titanium-based femoral head, (b) retrieved UHMWPE acetabular liner with an embedded titanium fibermesh piece, (c) qualitative mapping of location and brightness level of the worn regions under study.

- Regions covering more than 50% of the entire surface and visually having an intermediate brightness level. These regions noted moderately scratched (MS) are gray-colored in Fig. 1c.

2.2. Surface topography characterization of the retrieved femoral head

In this investigation, observations have been carried out by means of an optical microscope to obtain qualitative information about the magnitude of damage produced by scratching in these different regions. In each region, these qualitative observations have been combined to quantitative roughness measurements carried out by means of a three-dimensional contacting profilometer (KLA Tencor P10) having a 2 µm stylus radius. From the information related to those roughness measurements and reported in Table 1, it can be deduced that the selected experimental conditions correspond to a 1 µm horizontal resolution along a scanning trace and a $600 \times 600 \, \mu m^2$ size for each scanned area to which correspond a data file containing 120 000 points.

2.3. Roughness parameters under investigation

All the data files recorded in the four worn regions have been processed by a first specific computer algorithm to estimate the values of different implemented roughness parameters. The roughness parameters under investigation in this study are the same as those reported in the literature focusing on the topography characterization of orthopae-

Table 1
Experimental conditions used for each roughness measurement by means of the three-dimensional contacting profilometer

Acquisition rate	100 Hz
Speed rate	100 µm/s
Scanning length	600 µm
Space interval (y)	3 µm
Stylus force	2 mgf
Number of traces	200

dic bearing surfaces and cited in the introduction of this paper. This set of parameters $\{P_i; i \in [1 \text{ to } 13]\}$ included not only the parameters R_a, R_q, R_t, R_p, R_{pm}, S_k but also the parameters R_k, R_{pk}, R_{vk}, Mr_1, Mr_2, A_1, A_2 derived from the BAC (Abbott–Firestone curves) and defined in the guidelines of the DIN 4776 and ISO 13565-2 standards [14,15]. The amplitude parameters R_k, R_{pk} and R_{vk} are respectively called the core depth, the reduced peak height and the reduced valley depth. The definitions of all these roughness parameters of interest are reported in Appendix A.

For each processed data file related to a 3D roughness measurement which includes 200 scanning traces, the first step of the algorithm developed by the authors using the Turbo Pascal language consists in removing the spherical form of the femoral head (Fig. 2) and extracting the 200 resulting residuals profiles. In this study, the spherical form has been removed by means of a fitting second-order polynomial surface. The second step consists in calculating the values of the different implemented roughness parameters for each residual profile resulting from the first step;
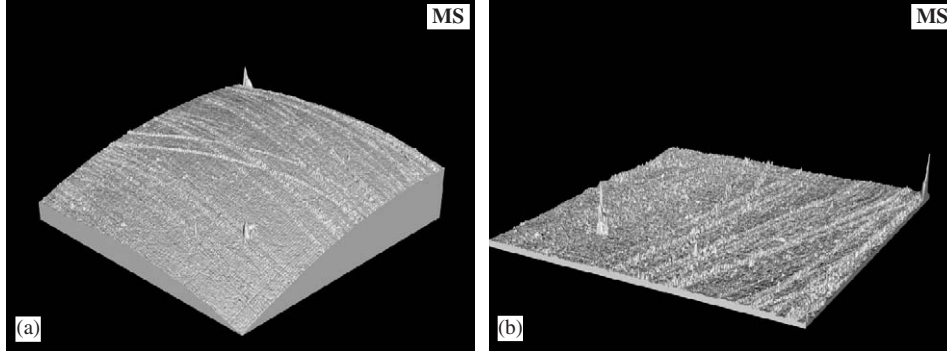
Fig. 2. (a) Visualization of an original data file recorded by means of the three-dimensional contacting profilometer in the region MS, (b) residual data file obtained after removing the spherical form at the first step of our computer algorithm.

200 values are therefore calculated for each roughness parameter P_i. Since 6 measurements have been carried in each region under investigation, a set of 1200 values is finally obtained per region after this second step and this for each roughness parameter P_i. For each region under investigation, this set is noted $\{P_{i,j}^{\text{Exp.}}; i \in [1 \text{ to } 13], j \in [1 \text{ to } 1200]\}_k$ with $k = \text{LS, MS, SSER, SSPR}$.

2.4. Relevance of roughness parameters under investigation

A second algorithm developed by the authors has been computed using the capabilities of the SAS (Statistical Analysis System) language. This algorithm enables to determine quantitatively, and without any preconceived opinion, the most relevant roughness parameter that discriminates the four worn regions LS, MS, SSER, SSPER. The integrated procedure of the ANOVA of the SAS language system has been used in a first step of the algorithm to calculate, for each roughness parameter under investigation P_i, the values of the treatment index F_i considering four classes corresponding to the four regions $k = \text{LS, MS, SSER, SSPR}$. This statistical index enables to rank the different implemented roughness parameters with regard to their ability of discriminating the four worn regions; a roughness parameter P_1 is considered to be more relevant than a parameter P_m if $F_1 > F_m$. However, it must be mentioned that the conventional statistical theory ANOVA does not take into consideration the fact that a small perturbation in any score of the experimental data set can influence the value of the calculated treatment index. In other words, the variability on the values F_1 and F_m have to be considered to affirm in a statistical sense that $F_1 \neq F_m$. For more details on the treatment index and the ANOVA, the reader should refer to [16].

To take into account the limitation previously cited, the ANOVA was combined to the CBBM in a second step of the algorithm with a view to providing a confidence level on the value of the treatment index. This second step had to be computed since the bootstrap theory is recent and is not integrated in the procedures of the SAS language. Briefly speaking, the CBBM is based on the mathematical resampling technique and it consists in generating a high number N of simulated bootstrap samples by perturbing the scores of a given experimental data set of size J. A bootstrap sample of size J indexed by $n(n \in [1 \text{ to } N])$, and noted $(x_1^{\text{Boot.}n}, x_2^{\text{Boot.}n}, \ldots, x_J^{\text{Boot.}n})$, is a collection of J values simply obtained by randomly sampling with replacement from the experimental data scores $(x_1^{\text{Exp.}}, x_2^{\text{Exp.}}, \ldots, x_J^{\text{Exp.}})$; each of them having a probability equal to $1/J$ to be selected. A bootstrap sample contains therefore scores of the experimental data set; some appearing zero times, some appearing once, some appearing twice, etc. For more details on the CBBM, the reader should refer to [17].

Fig. 3 shows the synoptic scheme of the combination CBBM/ANOVA that has been applied in this investigation. Such a combination enables an empirical probability density function (PDF) of N ($N = 1000$ in this study) simulated values $\{F_i^{\text{Boot.}n}; n \in [1, N]\}$ for each roughness parameter P_i to be plotted. Then, it is possible from each empirical PDF to extract the values of the mean, $\overline{F_i}$, as well as the percentile 5%, $F_i^{5\%}$, and the percentile 95%, $F_i^{95\%}$, that can be used to determine a 90% confidence level related to the roughness parameter P_i.

3. Experimental results

3.1. Conventional analysis of the topography

The qualitative information obtained on the topography by means of an optical microscope is summarized in Fig. 4. Only few isolated scratches are observed in the regions LS that visually have a bright finish meaning that the femoral head has only suffered a light degradation of its initial mirror finish in these regions. On the contrary, a severe degree of degradation consisting in a high density of large, deep and multidirectional scratches can be noticed in the regions SSPR and SSER visually having a low brightness level. Finally, a moderate degree of damage is noticed in regions MS which topography consists of a high density of numerous small and multidirectional scratches.

The quantitative information obtained on the topography by means of a three-dimensional contacting profilometer is summarized in Fig. 5. For each region k ($k = \text{LS, MS, SSER, SSPR}$), the mean and its associated

Experimental data related to the roughness parameter P_i :

$$(P_{i,1}^{Exp.}, P_{i,2}^{Exp.}, ..., P_{i,1200}^{Exp.})_{LS} \quad (P_{i,1}^{Exp.}, P_{i,2}^{Exp.}, ..., P_{i,1200}^{Exp.})_{MS}$$

$$(P_{i,1}^{Exp.}, P_{i,2}^{Exp.}, ..., P_{i,1200}^{Exp.})_{SSER} \quad (P_{i,1}^{Exp.}, P_{i,2}^{Exp.}, ..., P_{i,1200}^{Exp.})_{SSPR}$$

First Bootstrap data (n=1) on the experimental data :

$$(P_{i,1}^{Boot.1}, P_{i,2}^{Boot.1}, ..., P_{i,1200}^{Boot.1})_{LS} \quad (P_{i,1}^{Boot.1}, P_{i,2}^{Boot.1}, ..., P_{i,1200}^{Boot.1})_{MS}$$

$$(P_{i,1}^{Boot.1}, P_{i,2}^{Boot.1}, ..., P_{i,1200}^{Boot.1})_{SSER} \quad (P_{i,1}^{Boot.1}, P_{i,2}^{Boot.1}, ..., P_{i,1200}^{Boot.1})_{SSPR}$$

ANOVA on the First Bootstrap results related to the roughness parameter P_i : $F_i^{Boot.1}$

Repetition of the two precedent steps for n=2 to n=N=1000:
$$F_i^{Boot.2}, \ F_i^{Boot.3}, ..., F_i^{Boot.1000}$$

EMPIRICAL PDF OF F_i RELATED TO THE PARAMETER P_i :

(a)   ESTIMATION OF THE MEAN : $\overline{F_i}$

(b)   ESTIMATION OF THE PERCENTILE 5% : $F_i^{5\%}$

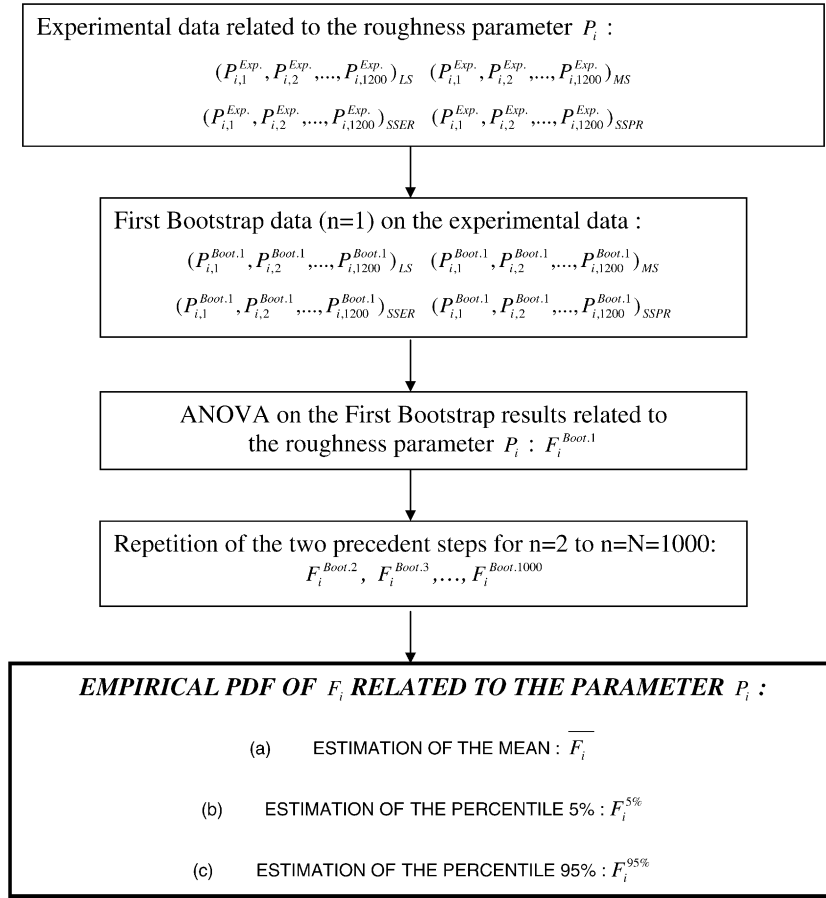(c)   ESTIMATION OF THE PERCENTILE 95% : $F_i^{95\%}$

Fig. 3. Synoptic scheme of the statistical treatment processed in this study for each roughness parameter $P_i (i \in [1 \text{ to } 13])$.
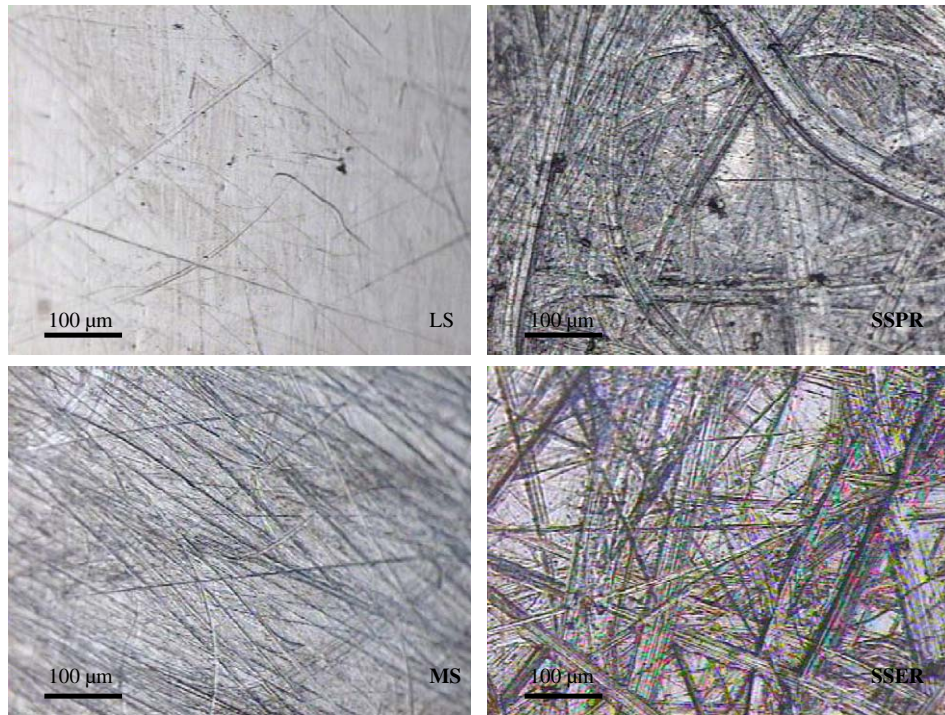

Fig. 4. Optical micrographs showing the characteristics of scratches in the four worn regions LS, MS, SSPR and SSER.
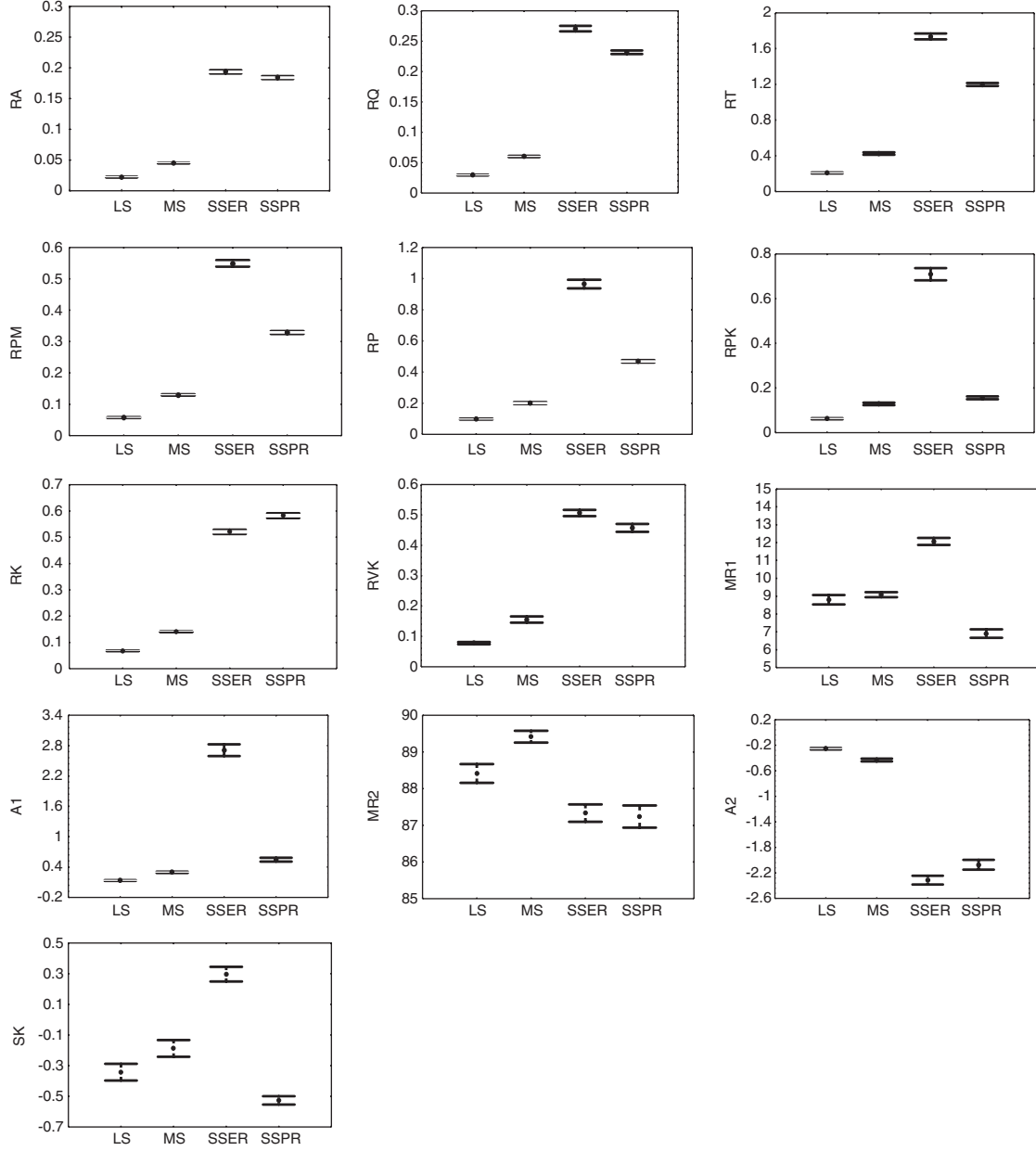
Fig. 5. Means and associated standard errors of the different roughness parameters under investigation for the different regions LS, MS, SSER and SSPR.

standard error are plotted for each element of the set $\{P_{i,j}^{\text{Exp.}}; i \in [1 \text{ to } 13], j \in [1 \text{ to } 1200]\}_k$; i.e. for each roughness parameter P_i under investigation. At first sight, it can be seen on this figure that all the values of the amplitude parameters $R_\alpha (\alpha = a, q, t, p, pm, k, pk, vk)$ tend to increase with the severity of damage degree if the overall regions are considered. This result physically reflect the expected fact that the height of the peaks and the depth of the valleys simply increase with the severity of damage.

It is also very interesting to notice on this figure that, while the values of the average amplitude parameters R_α $(\alpha = a, q, k)$ are of the same order for the two severely scratched regions SSER and SSPR, the values of the extreme-value parameters R_β $(\beta = p, \text{pm}, \text{pk}, t)$ are quite different as well as the values of the roughness parameters

Mr_1 and A_1; the values of all these parameters being always higher in the region SSER. Besides the values of the roughness parameters R_{vk}, Mr_2 and A_2 are of the same order for the two regions. These results physically mean that, while the regimes related to the core roughness and to the valleys lying below the core roughness are similar for the two severely scratched regions, the regime related to the peaks are significantly different; the peaks being higher in the region SSER than in the region SSPR. This result is confirmed by the interesting fact that, visualizing the topography of the measured areas by means of the three-dimensional contacting profilometer, some material build-up can be observed on either side of the large scratches crossing the region SSER whereas it is not the case for the region SSPR (Fig. 6).
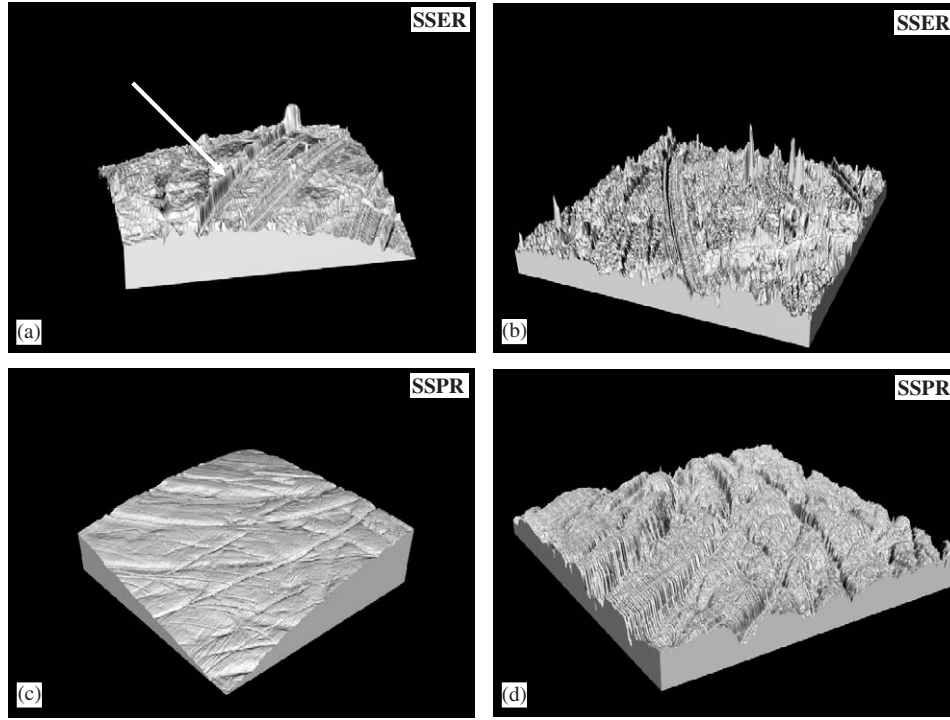
Fig. 6. Example of a typical area recorded by means of the three-dimensional contacting profilometer in region SSER (a) before and (b) after removing the spherical form: note the large scratch accompanied by material build-up marked with a white arrow. Example of a typical area recorded by means of the three-dimensional contacting profilometer in region SSPR (c) before and (d) after removing the spherical form: note the absence of peaks on either sides of the large scratches.

Finally, it is worth noting that, except for Mr_1 and Mr_2, the values of the means of the investigated roughness parameters are always significantly different for the different regions since there is no overlap of the standard bar errors. Unfortunately, there is no simple way to determine without preconceived opinion which of those investigated parameters is the most relevant to discriminate the topographies of the different regions. To solve this problem of major importance, it is proposed in this study to combine two statistical methods: for each roughness parameter, the conventional ANOVA is used to assess the value of the treatment index F and the CBBM to provide a confidence level on this value.

3.2. Relevance of roughness parameters

The relative relevance of the different investigated roughness parameters has been assessed considering four classes (related to the four investigated worn regions) during the statistical treatment as depicted in Fig. 3. Fig. 7 presents an example of three empirical probability density functions (PDF) of the treatment index F resulting from this statistical treatment in the case of the amplitude roughness parameters R_a, R_q and R_{pm}. At first sight, it can be seen on this figure that almost all the values of the treatment index related to the roughness parameter R_a are higher than those of the roughness parameters R_q and R_{pm}. This means that the amplitude roughness parameter R_a is
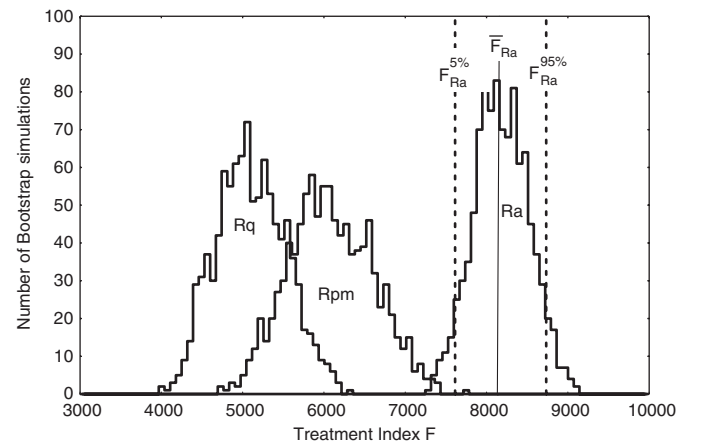

Fig. 7. Example of the empirical PDFs obtained by combination of ANOVA and CBBM in the case of the amplitude roughness parameters R_a, R_{pm} and R_q.

more relevant than the two latter ones for discriminating the topographies of the four investigated regions. Besides there is an overlap between the empirical PDFs of the amplitude roughness parameters R_q and R_{pm} meaning that the discriminating forces related to these parameters are not so different. From the empirical PDF of each roughness parameter, it is possible to assess the quantitative value of the mean of the treatment index $\overline{F}$ as well as the values of the percentiles $F^{5\%}$ and $F^{95\%}$ that enable to
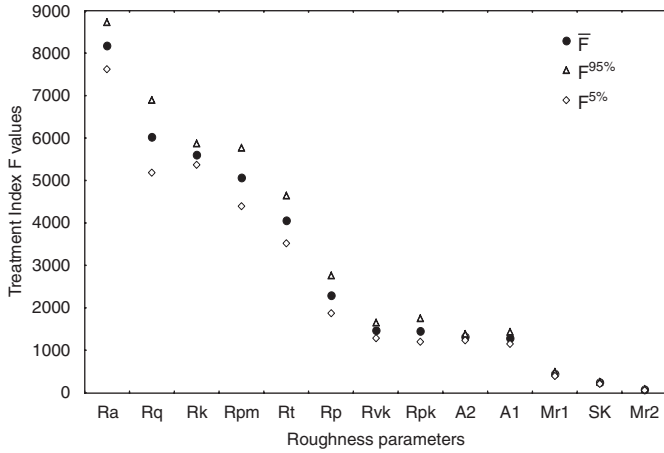
Fig. 8. Ranking of the roughness parameters under investigation according to the treatment index obtained when the four regions are considered in the ANOVA.
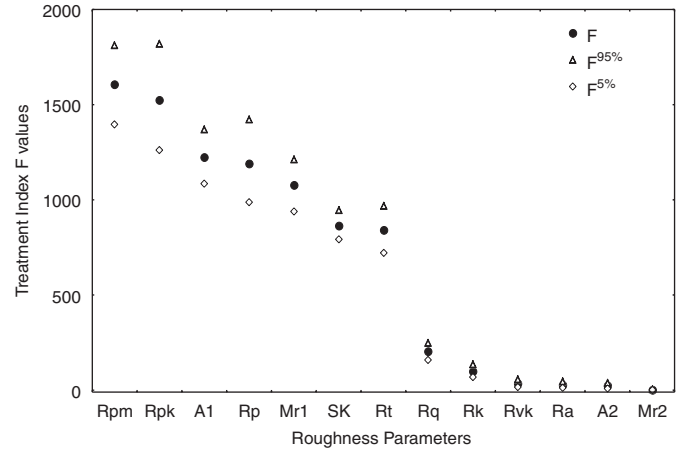

Fig. 9. Ranking of the roughness parameters under investigation according to the treatment index obtained when only the regions SSER and SSPR are considered in the ANOVA.

determine a 90% confidence level. The values of these usual statistical estimates are highlighted in Fig. 7 in the case of the arithmetic roughness R_a and reported in Fig. 8, which summarizes the results obtained for the overall investigated roughness parameters.

Fig. 8 shows that the highest values of the treatment index are recorded for the average amplitude parameters; the highest one being that of the arithmetic roughness parameter R_a. At the opposite, the least relevant parameters are those derived from the BAC and related to the regimes of peaks and valleys. Between these two populations of parameters are located the values of the extreme-value parameters. These results indicate that the average amplitude parameters are more relevant than the other ones for discriminating the different topographies of the four investigated worn regions; the most relevant of them being the arithmetic roughness parameter R_a. For information, the mean value of this parameter is respectively equal to 0.02, 0.05, 0.19 and 0.18 μm for the regions LS, MS, SSER and SSPR. Besides it can be noticed that several roughness parameters have equivalent discriminating forces, since there is an overlap of the 90% confidence levels associated to the mean values of their respective treatment index. This can be observed for example in the case of the set of parameters $\{R_q, R_k, R_{pm}\}$ or that of parameters $\{R_{vk}, R_{pk}, A_2, A_1\}$.

As it was shown in the conventional analysis, while the amplitude roughness parameters are quite similar for the regions SSER and SSPR, a high difference is observed for the extreme-value parameters related to the regime of peaks and for the skewness S_k of the ADF (Fig. 5). To complete the preliminary results of this conventional analysis, the statistical treatment depicted in Fig. 3 has been also applied taking into consideration only the two classes related to the worn regions SSER and SSPR; i.e. regions in which it has been qualitatively observed that the large scratches were accompanied by either some material build-up on their sides or not. Fig. 9 shows that the ranking

is completely different from that previously obtained by applying the same statistical treatment to the overall worn regions. In this case, it is worth noting that the arithmetic average roughness parameter R_a remains no more the most relevant parameter for discriminating the topographies of the regions SSER and SSPR. At the opposite, this latter one belongs to the group of the least discriminating parameters $\{R_q, R_k, R_{vk}, R_a, A_2, \mathrm{Mr}_2\}$, which includes all the average roughness parameters and the extreme-value ones related to the regime of valleys. In fact, this ranking simply indicates that, as expected, the most relevant parameters that should be used to discriminate the topographies of the regions SSER and SSPR are all the extreme-value parameters, which are sensitive to the height and the density of peaks. However, this ranking enables to conclude quantitatively and without any preconceived opinion that the most relevant of them are either R_{pm} or R_{pk}; these two parameters having the same discriminating force since there is an overlap of the 90% confidence levels related to the mean values of their respective treatment index. For information, the mean value of the parameter R_{pm} is respectively equal to 0.55 and 0.33 for the regions SSER and SSPR.

4. Discussion

In accordance with conclusions reported in other studies focusing on the effect of hard third bodies on the degradation of total hip prostheses components [3,4, 11,18], it is strongly believed that, in the present investigation, in vivo scratching of the titanium-based femoral head is the consequence of a deleterious abrasive third-body wear process due to the centimeter-length metallic fiber.

After migration from the fibermesh of the Harris–Galante Mark I metallic shell in which the UHMWPE was fixed, this fiber is thought to have entered in the equatorial region SSER from which it progressively and randomly moved towards the polar region SSPR. During its random

movements into the joint space, this fiber acted as a large-sized third body that is likely to have generated in a first time the numerous large scratches accompanied material build-up on either sides. After being embedded and fixed in its definitive position relatively to the UHMWPE acetabular liner, this hard third body is suspected to have participated for a second time to a continuously acting wear process due to its multiple passages over the region SSPR. In this region, this continuously acting wear process might have consequently eroded the material build-up (highest peaks) while leaving unaffected the deepest valleys of the large scratches previously generated during the random movement of the fiber into the joint space. This metal/metal friction between the centimeter-sized fiber and the femoral head occurring either in the region SSER or in the region SSPR is thought to have generated numerous metallic micrometer-sized wear debris. These debris could have acted themselves as small hard third bodies at the origin of the numerous or isolated small scratches respectively found in the regions MS and LS.

In accordance with the in vivo scratching mechanism previously described, the conventional analysis of the topography of the retrieved femoral head reveals that the values of all the investigated average amplitude parameters tend to increase with the severity of the damage observed in the considered worn region. The highest values of these parameters were therefore recorded in regions SSER and SSPR and the lowest ones in the regions MS and LS. Based on the combination of the ANOVA and the CBBM, the statistical treatment selected in this study indicates that, among all the studied roughness parameters, the average amplitude parameters are the most relevant ones for discriminating the different topographies of the four investigated worn regions; the most relevant of them remaining the almost universally used arithmetic roughness parameter R_a. It must be mentioned that, for the severely scratched regions SSER and SSPR, the related mean values of this parameter exceeds the upper limit tolerance of $0.05\,\mu m$ recommended in the standard ISO 7206–2 for the roughness of metallic femoral heads [19]. In regions LS and MS, the related mean values are respectively less and equal to this upper limit.

It is worth noting that the arithmetic roughness parameter R_a as the other average amplitude parameters fail to discriminate the topographies of the severely scratched regions SSER and SSPR if these latter regions are separately considered from the other ones. In accordance again with the in vivo scratching mechanism previously described, the conventional analysis of the femoral head also reveals that, while the values of the extreme-value parameters related to the regime of valleys are similar in these severely scratched regions, those related to the regime of peaks are higher for the equatorial region SSER than for the polar region SSPR. Based on the combination of the ANOVA and the CBBM, the statistical treatment indicates in this case that, among all the studied roughness parameters, the extreme-value parameters related to the regime of peaks are the most relevant ones for discriminating the different topographies of the regions SSER and SSPR; the most relevant of them being indifferently R_{pm} or R_{pk}. Looking at the mean values of these extreme-value parameters presented in Fig. 5, it can be concluded that the heights of the scratches detected in these regions are similar to those reported in other retrieval studies in which clinically relevant scratches on metallic femoral heads have been found to range from lower than $0.1\,\mu m$ to higher than $1\,\mu m$ [4,10,11]. In accordance with thoughts developed in these studies [4,7,11], it is also believed that the largest scratches accompanied by material build-up on either side have the highest contribution to the increased wear of the UHMWPE counterface although the effect of the smallest scratches cannot be ignored.

5. Conclusions

This study presents a generic methodology, which can help to determine quantitatively, and without any pre-conceived opinion, which relevant roughness parameter (s) should be used for assessing the surface topography of retrieved femoral heads. The conventional Analysis of Variance (ANOVA) and the Computer-Based Bootstrap Method (CBBM) were combined to rank the roughness parameters by calculating the values of the treatment index and a related confidence level for each of them.

Thanks to this methodology, it was shown that the arithmetic roughness parameter R_a was the most relevant to discriminate roughly the four scratched regions observed on a retrieved titanium femoral head damaged in the presence of a foreign third body during implantation. However, this average parameter, as the other average amplitude parameters, fails to discriminate finely the two most damaged of these regions; the first being located at the equator where the foreign body was thought to enter the joint space and the second being located at the pole where the foreign body randomly moved to reach its definitive fixed position. For these severely scratched regions, it was shown that the most relevant parameter was either the extreme-value parameter R_{pm} or R_{pk} that characterize the regime of peaks. The values of these peak parameters are statistically lower in the polar region than in the equatorial one. In the former region, the embedded and fixed foreign body participated to a continuously acting wear process that eroded the material build-up (highest peaks) while leaving unaffected the deepest valleys of the large scratches previously generated during the random movement of the fiber into the joint space. The methodology proposed in this paper enables a better understanding of the overall degradation mechanisms of the retrieved femoral head by a foreign third body.

Appendix A

Arithmetic roughness parameter R_a: Most commonly used amplitude roughness parameter for assessing the texture of orthopaedic bearing surfaces. This roughness parameter represents the area between the roughness and the reference mean line and it is defined as

$$R_a = \frac{1}{l} \int_0^l |z(x)| \, dx,$$

where l is the evaluation length and $z(x)$ is the profile height relative to the reference mean line at the position x.

Root mean square roughness R_q: Often used as an alternative to R_a, this amplitude roughness parameter is more sensitive to large deviations from the reference mean line. This parameter is defined as

$$R_q = \sqrt{\frac{1}{l} \int_0^l z^2(x) \, dx}.$$

Total amplitude roughness R_t: Extreme-value parameter measuring the distance between the highest peak and the lowest valley over the evaluation length.

Peak roughness R_p: Extreme-value parameter measuring the distance between the highest peak recorded over the evaluation length and the reference mean line.

Mean peak roughness R_{pm}: Extreme-value parameter measuring the mean distance between the highest peaks and the reference mean line in five consecutive sampling length. This average parameter is less prone to exceptional peaks than R_p.

Skewness S_k: Parameter measuring the global asymmetry of the ADF and indicating whether or not if there is a disproportionate number of high peaks or deep valleys. This parameter is defined as

$$S_k = \frac{1}{(R_q)^3} \int_{-\infty}^{+\infty} z^3(x) \, dx.$$

BAC parameters: Fig. A1 shows a schematic example of a BAC having a S-shape appearance as it is the case for many engineering surfaces. The horizontal axis represents the bearing area lengths as a percentage of the total assessment length of the profile and the vertical axis represents the heights of the profile. This figure also presents the roughness parameters R_k, R_{pk}, R_{vk}, Mr_1, Mr_2, A_1 and A_2 that can be derived from the BAC according to the guidelines mentioned in the DIN 4776 and ISO 13565-2 standards. The parameter R_k called the core depth is a measure of the height of the core material. The parameter R_{pk} called the reduced peak height is a measure of the portion of the protruding peaks above the core profile. The parameter R_{vk} called the reduced valley depth is a measure of the portion of deep valleys extending into the material
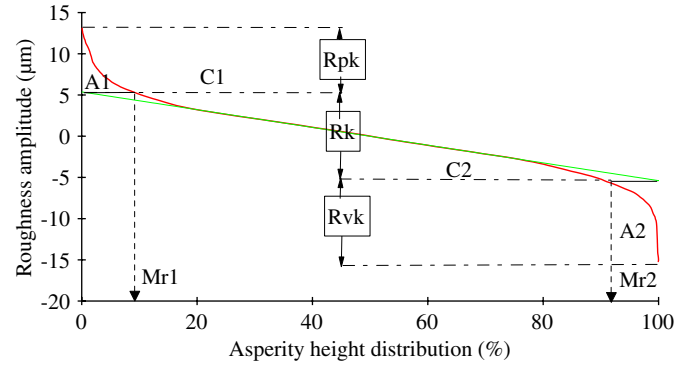

Fig. A.1. . Schematic representation of a bearing area curve as well as the related roughness parameters R_k, R_{pk}, R_{vk}, Mr_1, Mr_2, A_1, A_2.

below the core profile. The parameter Mr_1 is the lower limit of the core roughness and represents the material ratio at the transition between protruding peaks and core. The parameter Mr_2 is the upper limit of the core roughness and represents the material ratio at the transition between core and deep valleys. Finally the parameters A_1 and A_2 represent the 'area' portions related to the regimes of peaks and valleys, respectively.

References

[1] Hall RM, Unsworth A, Siney P, Wroblewski BM. The surface topography of retrieved femoral heads. J Mater Sci Mater Med 1996; 7:739–44.

[2] Hall RM, Siney P, Unsworth A, Wroblewski BM. The effect of surface topography of retrieved femoral heads on the wear of UHMWPE sockets. Med Eng Phys 1997;19:711–9.

[3] Brown TD, Stewart KJ, Nieman JC, Pedersen DR, Callaghan JJ. Local head roughening as a factor contributing to variability of total hip wear: a finite element analysis. J Biomech Eng 2002;124:691–8.

[4] McNie CM, Barton DC, Ingham E, Tipper JL, Fischer J, Stone MH. The prediction of polyethylene wear rate and debris morphology produced by microasperities on femoral heads. J Mater Sci Mater Med 2000;11:163–74.

[5] Tipper JL, Ingham E, Hailey JL, Besong AA, Fisher J, Wroblewski BM, et al. Quantitative analysis of polyethylene wear debris, wear rate and head damage in retrieved Charnley hip prostheses. J Mater Sci Mater Med 2000;11:117–24.

[6] Dowson D, El-Hady Diab MM, Gillis BJ, Atkinson JR. Influence of counterface topography on the wear of UHMWPE under wet and dry conditions. In: Lee LH, editor. Polymer wear and its control, American Society Series, Vol. 287, 1985. p. 171–87.

[7] Dowson D, Taheri S, Wallbridge NC. The role of counterface imperfections in the wear of polyethylene. Wear 1987;119:277–93.

[8] Wang A, Essner A, Polineli VK, Stark C, Dumbleton JH. Lubrication and wear of UHMWPE in total joint replacements. Tribol Int 1998;31:17–33.

[9] Elfick APD, Smith SL, Green SM, Unsworth A. The quantitative assessment of UHMWPE wear debris produced in hip simulator testing: the influence of head material and roughness, motion and loading. Wear 2001;249:517–27.

[10] Bowsher JG, Shelton JC. A hip simulator study of the influence of patient activity level on the wear of crosslinked polyethylene under smooth and roughened femoral conditions. Wear 2000;259:167–79.

[11] McNie CM, Barton DC, Ingham E, Tipper JL, Fischer J, Stone MH. Modelling of damage to articulating surfaces by third body particles in total joint replacements. J Mater Sci Mater Med 2000;11:569–78.

[12] Najjar D, Behnamghader A, Iost A, Migaud H. Influence of a foreign body on the wear of metallic femoral heads and polyethylene acetabular cups of total hip prostheses. J Mater Sci 2000;35: 4583–8.

[13] Najjar D, Bigerelle M, Migaud H, Iost A. Identification of mechanism of scratch generation on a retrieved metallic femoral head. Wear 2005;258:240–50.

[14] DIN 4776. Measurement of surface roughness parameters R_k, R_{pk}, R_{vk}, Mr_1, Mr_2 for the description of the material portion in roughness. Berlin, Germany, Mai, 1990.

[15] ISO13565-2. Geometrical product specification (GPS)—surface texture profile method; surface having stratified properties. Part 2: height characterisation using linear material ratio curve. Geneva, Switzerland, 1996.

[16] Keppel G, Sauffley WH. Introduction to design and analysis. New York: W.H. Freeman and Company; 1980.

[17] Efron B, Tibshirani R. An introduction to the bootstrap. New York: Chapman & Hall; 1993.

[18] Poggie Ra, Mishra AK, Davidson JA. Three-body abrasive wear behaviour of orthopaedic implant bearing surfaces from titanium debris. J Mater Sci 1994;5:387–92.

[19] ISO7206-2. Implants for surgery—partial and total hip joint prostheses—Part 2: articulating surfaces made of metallic, ceramic and plastics materials. Geneva, Switzerland, 1996.